

# Clinical recommendations of cardiac magnetic resonance, Part II: inflammatory and congenital heart disease, cardiomyopathies and cardiac tumors: a position paper of the working group 'Applicazioni della Risonanza Magnetica' of the Italian Society of Cardiology

Gianluca Pontone<sup>a</sup>, Gianluca Di Bella<sup>b</sup>, Castelletti Silvia<sup>c</sup>, Viviana Maestrini<sup>d</sup>, Pierluigi Festa<sup>e</sup>, Lamia Ait-Ali<sup>e</sup>, Pier Giorgio Masci<sup>f</sup>, Lorenzo Monti<sup>g</sup>, Gabriella di Giovine<sup>g</sup>, Manuel De Lazzari<sup>h</sup>, Alberto Cipriani<sup>h</sup>, Andrea I. Guaricci<sup>i</sup>, Santo Dellegrottaglie<sup>j</sup>, Alessia Pepe<sup>e</sup>, Martina Perazzolo Marra<sup>h</sup> and Giovanni Donato Aquaro<sup>e</sup>

The current document was developed by the working group on the 'application of cardiac magnetic resonance' of the Italian Society of Cardiology to provide a perspective on the current state of technical advances and clinical cardiac magnetic resonance applications and to inform cardiologists how to implement their clinical and diagnostic pathway with the introduction of this technique in the clinical practice. Appropriateness criteria were defined using a score system: score 1–3 = inappropriate (test is not generally acceptable and is not a reasonable approach for the indication), score 4–6 = uncertain (test may be generally acceptable and may be a reasonable approach for the indication but more research and/or patient information is needed to classify the indication definitively) and score 7–9 = appropriate (test is generally acceptable and is a reasonable approach for the indication).

**Keywords:** appropriateness criteria, cardiac magnetic resonance, cardiac tumor, cardiomyopathy, myocarditis, pericarditis

<sup>a</sup>UO Cardiologia, Centro cardiologico Monzino, Milano, <sup>b</sup>UO Cardiologia, Università di Messina, Messina, <sup>c</sup>IRCCS Istituto Auxologico Italiano, Milano, <sup>d</sup>Department of Cardiovascular, Respiratory, Geriatric, Anesthesiologic and Nephrologic Sciences, Sapienza University of Rome, Rome, <sup>e</sup>Fondazione G. Monasterio CNR-Regione Toscana, Pisa, Italy, <sup>f</sup>Centre Hospitalier Universitaire Vadois (CHUV), University Hospital Lausanne, Lausanne, Switzerland, <sup>g</sup>UO Radiologia Diagnostica, Humanitas Hospital, Rozzano (MI), <sup>h</sup>Clinica Cardiologica, Università degli Studi di Padova, Padua, <sup>i</sup>Unità Operativa di Cardiologia Universitaria Dipartimento di Emergenze e Trapianti di Organi (DETO) Azienda Ospedaliera Policlinico Consorziale di Bari, Bari and <sup>j</sup>Laboratorio di RM Cardiovascolare Divisione di Cardiologia Clinica Villa dei Fiori, Acerra, Italy

Correspondence to Giovanni D. Aquaro, MD, Fondazione G. Monasterio CNR-Regione Toscana, Pisa, Italy, Via Moruzzi, 1, 56124 Pisa, Italy  
 Tel: +39 050 3152824; e-mail: aquaro@ftgm.it

Received 21 June 2016 Revised 13 December 2016  
 Accepted 14 December 2016

J Cardiovasc Med 2017, 18:000–000

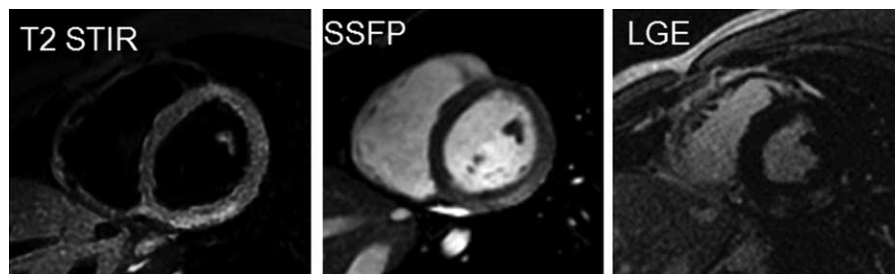
## Introduction

The current document was developed by the working group on the 'application of cardiac magnetic resonance (CMR)' of the Italian Society of Cardiology to provide a perspective on the current state of technical advances and clinical CMR applications and to inform cardiologists how to implement their clinical and diagnostic pathway with the introduction of this technique in the clinical practice. Appropriateness criteria were defined using a score system: score 1–3 = inappropriate (test is not generally acceptable and is not a reasonable approach for the indication), score 4–6 = uncertain (test may be generally acceptable and may be a reasonable approach for the indication but more research and/or patient information is needed to classify the indication definitively) and score 7–9 = appropriate (test is generally acceptable and is a reasonable approach for the indication).

## Inflammatory cardiac disease Myocarditis

Noninvasive diagnosis of myocarditis can be very difficult in clinical practice due to the high heterogeneity of the clinical presentations in absence of specific ECG and echocardiographic signs.<sup>1,2</sup> CMR is a valuable diagnostic tool to noninvasively diagnose myocarditis.<sup>3,4</sup> In 2009, the International Consensus Group on CMR in Myocarditis proposed 'Lake Louise Criteria' for myocarditis. At least two of the following CMR criteria must be present: increased of regional or global myocardial signal intensity in T2-weighted images (edema), increased global myocardial early (3 min) gadolinium enhancement ratio between myocardium and skeletal muscle in gadolinium-enhanced T1-weighted images (hyperemia), non-ischemic regional distribution in late gadolinium enhancement (LGE) most frequently involving the

Fig. 1



Cardiac MRIs of a case of ‘infarct like’ presentation of acute myocarditis. In T2-STIR image, myocardial hyperintensity of edema is found in inferior and inferolateral wall. In steady-state free precession images (SSFP), acquired early after gadolinium injection, hyperemia is detectable as well as positive LGE in the same myocardial regions.

subepicardial portion of the lateral left ventricular (LV) wall and less frequently the mid-wall of the interventricular septum.<sup>5</sup> The concomitant existence of skeletal muscle inflammation with edema, observed in acute myocarditis, can lead to false negative results for myocardial edema.<sup>6</sup> Hyperemia identification, as proposed by Lake Louise criteria, is very challenging and poorly used in the clinical setting. Recently, postcontrast cine steady-state free precession (SSFP) sequences were proposed as a new method for hyperemia identification (Fig. 1).<sup>7,8</sup> The sensitivity of CMR for the diagnosis of myocarditis is high for infarct-like presentation, low for myocarditis with heart failure and with arrhythmic clinical presentation. CMR findings should be used cautiously in these two latter conditions.<sup>9</sup> The persistence of inflammation in chronic myocarditis is associated with LV dilatation and dysfunction and to tissue abnormalities on CMR,<sup>1</sup> but the role of CMR in assessing chronic myocarditis patients is uncertain. Recent data suggest that chronic myocardial inflammation may be associated with generalized myocardial edema and to an increase of global myocardial enhancement.<sup>10,11</sup> Recent reports demonstrated that hyperenhancement areas can decrease or even disappear over time.<sup>12,13</sup> A study of comparison with endomyocardial biopsy (EMB) demonstrated that CMR with LGE is highly accurate to detect acute myocardial inflammation, in which LGE is positive in 95% cases, but it is not sensitive to detect chronic myocarditis (LGE positive in only 40%).<sup>14,15</sup> CMR may be considered as an appropriate diagnostic tool in hemodynamically stable patients with suspected acute myocarditis (Table 1).<sup>1</sup> Based on the different prognosis for acute myocarditis with different clinical and instrumental presentations, endomyocardial biopsy should be reserved in patients with clinical worsening despite pharmacological treatment, and it should be preferred with respect to CMR in unstable patients.<sup>16</sup> Preliminary data suggest that the early use of CMR reduces hospitalization time and costs.<sup>17</sup>

### Pericarditis

Pericardial abnormalities observed in pericarditis (effusion, acute or chronic inflammation) can be easily identified by CMR.<sup>18</sup> T1-weighted fast spin echo (FSE) allows the distinction between transudative (hypointense) and exudative (hyperintense) pericardial effusion. SSFP images allow detection of fluid (hyperintense) or dense exudation (intermediate intensity). Finally, T2-weighted imaging permits visualization of edema of the inflamed pericardial layers (hyperintense layers). At LGE, hyperintensity of pericardial layers is caused by the presence of active inflammation with granulomatous tissue, edema and neoangiogenesis.<sup>19</sup> In chronic recurrent pericarditis, CMR-guided therapy is associated with a reduction of recurrences.<sup>20</sup>

Acute pericarditis may evolve in chronic inflammation and/or constrictive pericarditis. The thickening of pericardial layers is the typical morphological finding in constrictive pericarditis: a thickness more than 4 mm is suggestive for pericardial constriction, whereas more than 5–6 mm had high specificity for pericardial constriction.<sup>21,22</sup> Other morphofunctional abnormalities of constriction are right ventricular (RV) tubular shape, dilated atria, dilated caval/hepatic veins, septal bouncing and/or shift in early diastolic ventricular filling on real-time cine CMR during inspiration due to decreased pericardial compliance.<sup>22</sup> CMR has also the advantage to differentiate between atypical forms of constriction as transient constriction (with demonstration of active inflammation in T2-weighted images and LGE) and effusive-constrictive forms (with combined effect of focal constriction and pericardial effusion) that may resolve after appropriate therapy.<sup>23</sup>

### Nonischemic cardiomyopathies

#### Dilated cardiomyopathy

CMR is the gold standard technique to assess ventricular volumes, mass and functional parameters as stroke

**Table 1** Appropriateness criteria for inflammatory heart disease

	Appropriateness score	ESC guidelines class of indication	Pulse sequences
Suspected acute myocarditis in hemodynamically stable patient and nonobstructive CAD	9	–	Cine-bSSFP in short-axis views T2 STIR in short-axis views Early enhancement T1 FSE LGE in short-axis views
Suspected acute myocarditis in nonhemodynamically stable patient and nonobstructive CAD	2	–	As above
3–6 months CMR follow-up for evaluation of myocardial edema and LGE	6	–	Cine-bSSFP in short-axis views T2 STIR in short-axis views LGE in short-axis views
Confirmation and characterization of pericardial effusion	4	Ia C indicated for loculated pericardial effusion, pericardial thickening and masses, as well as associated chest abnormalities	Cine-bSSFP in short-axis and long-axis views T2 STIR in short-axis and long-axis views T1 FSE in short-axis and long-axis views LGE in short-axis and long-axis views
Acute pericarditis	6	I C second-level testing for diagnostic work-up in pericarditis. Evaluation of myocardial involvement	As above
Chronic or recurrent pericarditis	8	–	As above
Suspect of constrictive pericarditis	9	I C to assess pericardial thickness, degree and extension of pericardial involvement	Cine-bSSFP in short-axis and long-axis views Real-time cine in short-axis views T2 STIR in short-axis and long-axis views T1 FSE in short-axis and long-axis views LGE in short-axis and long-axis views

CAD, coronary artery disease; CMR, cardiac magnetic resonance; FSE, fast spin echo; STIR, Short-Tau Inversion Recovery. Appropriateness criteria: 1-3 inappropriate; 4-6 uncertain; 7-9 appropriate.

volume and ejection fraction. In patients with newly diagnosed LV dysfunction, the pattern of presentation of LGE is very accurate to predict the ischemic and nonischemic cause.<sup>24</sup> In the ischemic LV dysfunction, LGE is confluent, with constant involvement of subendocardium and with a coronary-related regional distribution.<sup>25,26</sup> In the nonischemic-dilated cardiomyopathy (NIDCM), LGE is absent or distributed as a mid-wall stria, patchy or with a subepicardial distribution. Several studies investigated the role of LGE as a predictor of adverse remodeling and worse prognosis. The prevalence of LGE in NIDCM is 25–28% and is associated with increased risk of all-cause mortality and hospitalization for heart failure.<sup>27,28</sup> The strongest additive value of LGE is to identify patients at risk for sudden cardiac death (SCD): LGE is associated with an increased risk of SCD/aborted SCD of more than five times compared with patients without, having an additive value to ejection fraction for the identification of patients suitable for primary prevention implantable cardioverter defibrillator.<sup>28–30</sup>

### Arrhythmogenic cardiomyopathy

The diagnosis of arrhythmogenic RV cardiomyopathy (ARVC) is challenging, and it is based on a group of structural, histologic, ECG and family history criteria, proposed and modified by a dedicated task force in 2010 (Table 2).<sup>31</sup> CMR takes part of these criteria for the qualitative evaluation of regional wall motion (akinesia, dyskinesia or dyssynchronous contraction) and global quantification of RV size and systolic function with specific cutoff values. A major criterion is fulfilled in presence of regional RV akinesia or dyskinesia or

dyssynchronous RV contraction combined with RV end-diastolic indexed volume (EDVi) at least 110 ml/m<sup>2</sup> (man) or at least 100 ml/m<sup>2</sup> (woman) or with a RV ejection fraction 40% or less; a minor criterion is satisfied when regional RV akinesia or dyskinesia or dyssynchronous RV contraction is combined with a ratio of RV EDVi at least 100 to less than 110 ml/m<sup>2</sup> (man) or at least 90 to less than 100 ml/m<sup>2</sup> (woman), or with a RV ejection fraction more than 40 to 45% or less. To better visualize wall motion abnormalities, the study of the RV should include short-axis, transaxial stack of cines and long-axis images. Tissue characterization should be preferably performed using FSE sequences, acquired in the axial and short-axis planes for best RV free wall and RV outflow tract evaluation. Identification of fat in the RV, as disruption of the smooth interface between epicardial surface and RV wall (evaluated in FSE images with and without fat saturation), and detection of fibrosis (using LGE technique) are not part of the current task force criteria, because of lack of specificity, high interobserver variability, as well as some technical limitations, due to the thin RV wall thickness.<sup>32–36</sup> LV abnormalities (diffuse or regional LV dysfunction, mid-wall or subepicardial LV LGE) are not uncommon in ARVC patients and may represent more advanced stages of the disease.<sup>35</sup> However, many concerns were raised about new CMR criteria.<sup>37</sup> In fact, quantitative cutoff for task force criteria were derived from the MESA study. In the MESA study, ventricular volume was measured using the obsolete fast gradient echo pulse sequence, instead of the widely used SSFP sequences.<sup>38</sup> SSFP images provide superior contrast between blood and endocardium, with less blood flow dependence.<sup>39,40</sup> Also, the revised task force criteria

**Table 2** Cardiomyopathies, dilated cardiomyopathy and arrhythmogenic right ventricle cardiomyopathy

	Appropriateness score	ESC guidelines class of indication	Pulse sequences
<b>NIDCM</b>			
Assessment of LV/RV mass, volumes, EF and stroke volumes	9	I C, CMR is recommended to evaluate cardiac structure and function, to measure LV EF especially in patients with inadequate acoustic window or in which echo is inconclusive or incomplete	Cine-bSSFP in short-axis views from mitral valve to apex
Monitoring cardiac function following therapy	6	–	Cine-bSSFP in short-axis views from mitral valve to apex
Differential diagnosis between ischemic and nonischemic DCM in newly diagnosed LV dysfunction	9	–	LGE in short-axis views and radial slices
Functional and tissue evaluation in patient with indication of ICD/CRT	8	IIb C, CMR for demonstration of myocardial fibrosis that is indicator of increased risk of sudden death in inflammatory disease	Cine-bSSFP in short-axis views from mitral valve to apex LGE in short-axis views and radial slices
CMR with LGE for the prediction of response to therapy	7	–	LGE in short-axis views
<b>ARVC</b>			
Cause of RV dilation or dysfunction	8	–	Cine-bSSFP in short-axis views from mitral valve to apex $Q_p/Q_s$ evaluation with VEPC
Identification of biventricular tissue and wall motion abnormalities in patients with ventricular arrhythmias	7	–	Cine-bSSFP in short-axis and long-axis views FSE in short-axis and long-axis views LGE in short-axis and long-axis views
Follow-up CMR in patients with tissue abnormalities or wall motion abnormalities or RV dilatation, not satisfying TF criteria	7	–	As above
CMR in mutation carries or familiar of a ARVC proband	7	–	As above

ARVC, arrhythmogenic right ventricle cardiomyopathy; ICD, implanted cardioverter defibrillator; CRT, cardiac resynchronization therapy; bSSFP, balanced steady state free precession; LGE, late gadolinium enhancement; CMR, cardiac magnetic resonance; DCM, dilated cardiomyopathy; EF, ejection fraction; FSE, fast spin echo; LV, left ventricle; NIDCM, nonischemic-dilated cardiomyopathy; VEPC, velocity encoded phase contrast; RV, right ventricle; TF, task force criteria. Appropriateness criteria: 1-3 inappropriate; 4-6 uncertain; 7-9 appropriate.

used MESA patients whose mean age was 60 years, whereas ARVC patients were 20–30 years younger on average. This point is quite relevant because RV end-diastolic volume decreased 4.6% per decade in healthy controls.<sup>38</sup>

Yet, recent evidence suggests that LV involvement in ARVC is very frequent and associated with higher risk or arrhythmic events. Notwithstanding, LV involvement is not mentioned in the task force criteria for CMR.

Moreover, despite the fact that fat infiltration, LGE and LV involvement detected by CMR were not included in current task force criteria, they remain important findings of CMR in ARVC, with a demonstrated prognostic relevance<sup>41,42</sup> (Fig. 2).

### Cardiac amyloidosis

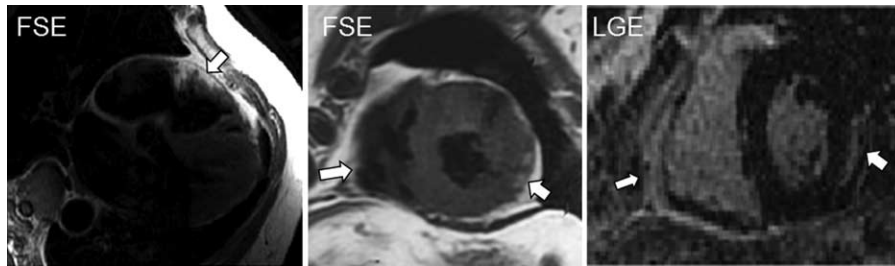
The presence and severity of cardiac involvement in immunoglobulin light-chain and transthyretin amyloidosis are crucial for prognosis and therapeutic options.<sup>43–45</sup> CMR represents a good alternative to echocardiography to evaluate morphology and function and to depict a broader range of differences between the two main

amyloidosis types.<sup>46–48</sup> LGE technique has an excellent diagnostic accuracy for the diagnosis of cardiac amyloid. The ‘typical’ pattern of LGE consisting in a diffuse subendocardial enhancement with a noncoronary distribution, coupled with abnormal gadolinium kinetics of myocardium and blood pool (early darkening of blood pool, nulling defect of myocardium) are pathognomonic of cardiac amyloidosis (Fig. 3a).<sup>49–51</sup> However, some variants of this typical LGE pattern may sometimes be found, presenting with localized, transmural or patchy enhancement. LGE may also involve RV myocardium and atrial walls.<sup>52–54</sup>

Up to now, a standardized LGE approach to detect cardiac amyloid infiltration is lacking, and in the early stage of cardiac involvement LGE may be negative. Accordingly, the presence of a negative LGE should not exclude cardiac amyloid when pretest probability is high.<sup>55</sup> Phase-sensitive inversion recovery sequences are under evaluation as an operator-independent alternative to the standard LGE technique.<sup>56</sup>

Similarly, the measurement of native T1 and extracellular volume (ECV) are promising techniques for the early

Fig. 2



A case of arrhythmogenic right ventricular cardiomyopathy. Fast spin echo images shows fat infiltration in the subtricuspidal wall and in lateral free wall of right ventricle as well in left lateral wall. In the same region, LGE is also positive in the same regions.

diagnosis of cardiac amyloids.<sup>57–61</sup> However, further and larger studies are needed to confirm preliminary results.

### Hypertrophic cardiomyopathy

Over the last decade, CMR has emerged as an important imaging technique to provide additional information to characterize the broad spectrum of phenotypic expression of this complex disease due to its high spatial resolution, ability to obtain images in any plane and clear definition between the interface of blood pool and myocardium. Therefore, its diagnostic role is particularly relevant in patients with suboptimal images from echocardiography as established by ACC/AHA and by the more recent ESC guideline for the diagnosis and treatment of hypertrophic cardiomyopathy (HCM) (Class I, level B) (Table 3).<sup>62,63</sup>

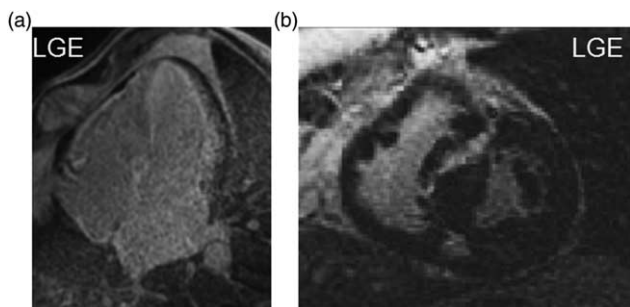
CMR provides precise wall thickness measurements in any location of the LV and RV and is superior to echocardiography to detect focal hypertrophy limited to anterior wall or apex, apical aneurysms.<sup>64–69</sup> Cine images of 5 mm thickness may improve the yield of detection of microaneurysm and crypts. The guidelines suggest to

consider CMR in suspected cases of apical hypertrophy or aneurysm (Class IIa, level C).<sup>63</sup>

In genotype-positive phenotype-negative patients, CMR can show subtle phenotypic markers of the disease including papillary muscles abnormalities, myocardial crypts, elongated leaflets of the mitral valve and increased myocardial trabeculae.<sup>70–78</sup> CMR has been also used to evaluate the consequence of septal alcohol ablation and myectomy.<sup>79–81</sup>

Lastly, CMR should be considered to evaluate the presence, the distribution and the extent of myocardial fibrosis that may help to distinguish among differential diagnosis (for example from cardiac amyloidosis or from secondary hypertrophy) and phenotype (Fig. 3b). Multiple studies reported high prevalence of LGE in HCM, predominantly as a patchy mid-wall pattern involving areas of hypertrophy or at the RV insertion points.<sup>82–84</sup> Some studies reported a relationship between LGE and cardiac outcome in HCM patients,<sup>85–88</sup> and a recent multicenter study demonstrated that the extent of LGE at least 15% of LV mass was associated with worse prognosis.<sup>89</sup> However, LGE is not yet considered a major risk marker of SCD by current ESC guidelines.

Fig. 3



LGE images are useful for the differential diagnosis between cardiac amyloidosis (a) and hypertrophic cardiomyopathy (b). In cardiac amyloidosis, LGE image shows diffuse subendocardial enhancement and early darkening of blood. In hypertrophic cardiomyopathy, LGE image shows focal intramural fibrosis in the hypertrophied septum.

### Anderson–Fabry disease

LV hypertrophy is a common cardiac manifestation in Anderson–Fabry disease (AFD). Differential diagnosis of AFD versus other causes of LV hypertrophy and detection of early cardiac involvement is important given existing specific replacement enzyme therapy.

CMR provides complementary data to echocardiography in AFD especially through its ability to identify tissue characterization. LGE is a frequent finding in AFD patients and is located particularly in the basal inferolateral LV wall.<sup>90–92</sup>

Recently, preliminary results suggest that the T1 mapping technique held the potentiality to discriminate AFD (low myocardial T1) among patients with LV hypertrophy and to detect early stage.<sup>93–95</sup> Further larger studies are required to support these findings.

Table 3 Cardiomyopathies, hypertrophic cardiomyopathy and others

	Appropriateness score	ESC guidelines class of indication	Pulse sequences
<b>HCM</b>			
Assessment of LV mass, wall thickness	8	I C, CMR in patients suspected for HCM with inadequate acoustic window IIa B, in all HCM patients	Cine-bSSFP in short-axis and long-axis views
Assessment of LVOT dynamic obstruction	5	–	Cine-bSSFP in oblique long-axis view (3-chamber view) LGE in short-axis views
Identification and quantification of myocardial fibrosis with LGE	9	IIa B, CMR with LGE in all patients IIb C, CMR with LGE every 5 years in clinical stable patients, every 2–3 years in patients with progressive disease	LGE in short-axis views
Differential diagnosis among HCM, amyloidosis and Fabry disease	9	IIa C, CMR in patients with suspected cardiac amyloidosis	LGE in short-axis views  T1 mapping
Evaluation of outflow tract after myectomy	5	–	ECV Cine-bSSFP in oblique long-axis view (3-chamber view)
<b>Hemochromatosis</b>			
Initial screening of iron overload at first diagnosis	9	–	Multiecho T2* GRE in short-axis view
Annual follow-up in patients with myocardial T2 < 20 ms	9	–	As above
2-year follow-up in patients with myocardial T2 ≥ 20 ms	9	–	As above
<b>Noncompaction</b>			
Confirmation of echocardiographic suspicion	7	–	Cine-bSSFP in short-axis and long-axis views Cine-bSSFP in short-axis and long-axis views
<b>Sarcoidosis</b>			
Screening of myocardial involvement in patients with systemic sarcoidosis	7	–	LGE in short-axis views and long-axis views

CMR, cardiac magnetic resonance; ECV, extracellular volume; HCM, hypertrophic cardiomyopathy; LVOT, left ventricular outflow tract; LV, left ventricle. Appropriateness criteria: 1-3 inappropriate; 4-6 uncertain; 7-9 appropriate.

### Hemochromatosis

Iron overload cardiomyopathy (IOC) results from the accumulation of iron in the myocardium mainly due to genetic disorders of iron metabolism or multiple transfusions (such as in thalassemia). Heart failure secondary to iron overload remains one of the main causes of mortality in IOC. However, IOC can be reversed by chelation therapy.<sup>96</sup> The highly sensitive and reproducible CMR T2\* technique has revolutionized IOC management, providing for the first time a direct, noninvasive, quantitative assessment of cardiac iron deposit<sup>97</sup> for first diagnosis and for the titration of iron chelation therapy.<sup>98</sup> Specifically, the multislice approach<sup>99</sup> can detect the uneven iron accumulation in the heart and allows identification of patients at risk for cardiac complications in a precocious stage.<sup>100</sup> A T2\* value less than 20 ms is considered the conservative cutoff for segmental and global heart iron. The first cardiac T2\* assessment should be performed as early as possible without sedation in patients with hemochromatosis.<sup>101</sup> Moreover, due to the multifactorial etiopathogenesis of cardiomyopathy in hemochromatotic patients, it is recommended a multiparametric CMR approach by a conventional evaluation

of cardiac function, myocardial fibrosis by LGE technique<sup>102</sup> and edema when myocarditis is suspected.

### Noncompaction cardiomyopathy

LV noncompaction cardiomyopathy (LVNC) is a primary genetic cardiomyopathy characterized by the presence of an extensive noncompacted myocardial layer lining the cavity of the LV, probably due to a failure of trabecular remodeling during embryogenesis with the persistence of multiple, prominent ventricular trabeculae separated by deep intertrabecular recesses.<sup>103</sup>

After the first echocardiographic suspicion, CMR is recommended to confirm the morphological diagnostic criteria. Petersen *et al.*<sup>104</sup> reported that the finding of a ratio of more than 2.3 between the thickness of the noncompacted and compacted myocardial layers in diastole at least at one myocardial segment is diagnostic. However, these criteria have reduced specificity particularly when used in a population with low pretest probability of LVNC. More complex diagnostic criteria are currently under evaluation.<sup>105,106</sup> Patients with HCM or carriers of sarcomeric mutation may present with a

phenotype of LVNC. In these cases, CMR may help to differentiate between HCM with focal noncompaction from LVNC. The prognostic role of isolated noncompaction without LV dysfunction or reduced wall thickness is still debated. Nowadays mid-wall LGE is the only demonstrated CMR-based marker of worse prognosis in this cardiomyopathy.<sup>107</sup>

### Sarcoidosis

Sarcoidosis is a systemic granulomatous disease involving the heart in 20–30% of the cases at autopsy.<sup>108</sup> Because of the focal myocardial involvement, endomyocardial biopsy yields low sensitivity. Moreover, most noninvasive diagnostic techniques have a low sensitivity and specificity. CMR is able to detect all phases of the pathological features of cardiac sarcoidosis characterized by noncaseating epitheloid granulomatous infiltration: focal wall thickening in cine images, edema on T2-Short Tau Inversion Recovery (STIR) images, gadolinium enhancement on early and late images.<sup>109,110</sup> CMR is also able to assess the response of the inflammation to immunosuppressive treatment that can improve the prognosis. Unfortunately, CMR cardiac findings in sarcoidosis are nonspecific and can be found in myocarditis, in cardiac lymphoma and mimic myocardial infarction. Moreover, CMR can evaluate impairment of cardiac function, pericardial effusion and hilar or mediastinal lymphadenopathy.

### Chagas cardiomyopathy

In Chagas cardiomyopathy, CMR can be used as an accurate and detailed assessment of the ventricular volumes, function and segmental contractility. CMR is also able to detect complications as ventricular aneurysms with parietal thinning and the presence of intracavitary thrombus. Reparative fibrosis is characteristic of this cardiomyopathy and is believed to be responsible for many aspects of its poor prognosis. Fibrosis is related to severe ventricular arrhythmias, heart failure, sudden death and other major events. CMR with LGE technique allows detection and quantification of myocardial fibrosis. T1 and T2 mapping are under evaluation for the identification of early myocardial involvement.

### Cardiotoxicity

Chemotherapy-induced cardiotoxicity shows an increasing incidence and represents a significant determinant of quality of life and mortality during ongoing treatment and in long-term survivors of cancer. Echocardiography remains the most used method to monitor cancer patients, but CMR is a valid second-line imaging modality (Table 4).

Based on the recent joint consensus document of the EACVI/ASE, the use of CMR in the clinical setting is strictly recommended for quantification of LV ejection fraction when the quality of echocardiogram is suboptimal; confirming a LV ejection fraction less than 53% by

echocardiogram; during the follow-up, for the LV ejection fraction quantification in cases of possible discontinuation of chemotherapy; and when LV ejection fraction estimation by echocardiogram is controversial.<sup>111</sup>

Anyway, the CMR incremental value is also for detecting early cardiac injury, quantifying RV function and cardiac mass, and monitoring chemotherapy-treated patients over time, whose management depends on minimal variations in biventricular function parameters.

### Takotsubo cardiomyopathy

Takotsubo cardiomyopathy (TTC), called also 'stress-induced cardiomyopathy' and/or 'transient LV apical ballooning syndrome', is an acquired cardiomyopathy characterized by transient regional wall motion abnormalities (usually in mid-apical segments of LV) not related with stenosis of a coronary artery, that is provoked by pronounced negative emotional, psychological or physical stress. CMR should be considered for the differential diagnosis between TTC and acute coronary syndrome. The typical CMR findings in TTC are regional wall motion abnormalities in apical and mid-LV segments added with a possible presence of global LV dysfunction and/or LV dilatation, myocardial edema detected using T2-W images in apical and mid-LV segments, absence of myocardial LGE (mild-intensity LGE described 10–40% of cases and related to interstitial edema), and resolution at 3 months of CMR abnormalities.<sup>112,113</sup>

### Cardiac transplantation

The mainstays of posttransplant graft surveillance are echocardiography, coronary angiography and endomyocardial biopsy providing assessment of cardiac function and detection of manifestations of both acute rejection and cardiac allograft vasculopathy. CMR may be used in patients with inadequate acoustic window to evaluate cardiac function and volumes. Its higher reproducibility permit identification of early changes in ventricular volume and minimal decrease of ejection fraction as well as the acute increment of LV mass. Myocardial T1 and T2 are increased in the acute phase following transplantation, then T2 shortens. Several studies demonstrated that an increase of myocardial T2 (60 ms) is highly predictive of acute rejection. LGE may present subepicardial enhancement but it is not sensitive. T1 mapping and ECV measurement are currently under study for the evaluation of acute rejection. The use of CMR stress perfusion with vasodilators is sensitive to detect severe cardiac allograft vasculopathy but its accuracy drops significantly in the presence of mild disease when compared with coronary angiography.

### Cardiac tumors and pseudotumors

Primary cardiac tumors can occur in all age groups and are rare, with an estimated cumulative prevalence of 0.002–

Table 4 Cardiac toxicity and tumors

	Appropriateness score	ESC guidelines class of indication	Pulse sequences
Cardiotoxicity			
Functional evaluation in patients with suboptimal acoustic window or with LV dysfunction by echo	9	–	Cine-bSSFP in short-axis views
Screening and follow-up in all patients with risk factors for cardiotoxicity	5	–	Cine-bSSFP in short-axis views T1 mapping, ECV, and T2 mapping LGE in short-axis views
Cardiac tumors			
Cardiac mass characterization (location, size, functional impact, relation with extracardiac structures and tissues properties)	9	–	Cine-bSSFP in short-axis and long-axis views T2 FSE and/or STIR in short-axis and long-axis views T1 FSE in short-axis and long-axis views First-pass perfusion T1 FSE at 1–3 min following Gd LGE in short-axis and long-axis views
Differential diagnosis between mass and pseudomass	9	–	As above
Differential diagnosis between benign and malign tumors	7	–	As above
Differential diagnosis between intracavitary thrombi and tumors	9	–	As above
Tissue characterization of small mobile cardiac masses (papillary fibroelastomas and valve vegetations)	2	–	As above

ECV, extracellular volume; bSSFP, balanced steady state free precession; LGE, late gadolinium enhancement; ECV, extracellular volume; FSE, fast spin echo; LV, left ventricle. Appropriateness criteria: 1-3 inappropriate; 4-6 uncertain; 7-9 appropriate.

0.3% at autopsy.<sup>112</sup> Approximately 75% are histologically benign, and the most common are myxomas, papillary fibroelastomas, lipomas and hemangiomas in the adult population, rhabdomyomas, fibromas and teratomas in children. Almost all malignant primary cardiac tumors are sarcomas, with angiosarcoma being the commonest in adults and rhabdomyosarcoma in children. In autopsy studies, metastatic involvement of the heart (mainly from bronchogenic carcinoma, lymphoma/leukemia and carcinomas of the breast and esophagus) is largely more prevalent than primary cardiac tumors.<sup>113</sup>

Dark and bright blood images in the axial, coronal and sagittal planes covering the entire chest and base to apex short-axis and long-axis views should be included in the CMR study. Considering its wide availability and convenience, echocardiography is typically the first-line modality in assessing patients with cardiac masses, but CMR is required to obtain a complete noninvasive characterization. In some cases, cardiac computed tomography (CT) is also included in the diagnostic work-up.

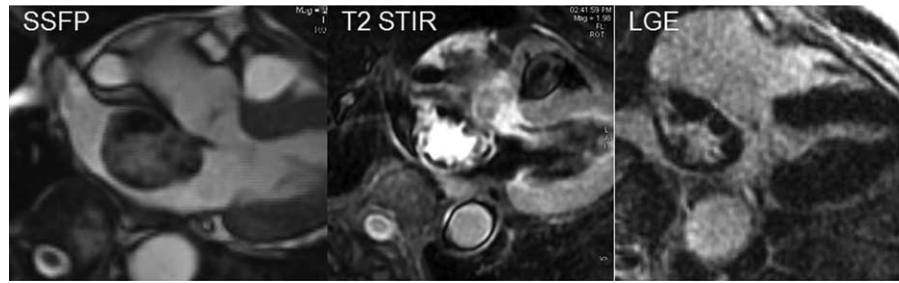
CMR images allow the definition of any cardiac mass in terms of location, size, extension, motility, hemodynamic impact, tissue characteristics and signs of malignancy. Tissue characteristics can be inferred from signal properties assessed on images obtained with different scan

sequences. A typical imaging protocol for the study of cardiac masses with CMR includes cine images (SSFP), precontrast morphologic images (T1-weighted FSE with and without fat saturation; T2-weighted FSE with fat saturation), and postcontrast images (first-pass perfusion module and late gadolinium enhancement module).<sup>114</sup> The identification of the nature of a mass involving the heart is reached by combining information about location, morphology and signal characteristics (Fig. 4).

Benign cysts represent a common incidental finding on CMR studies and are frequently detected at the pericardial level. Pericardial cysts appear as fluid-filled well demarcated structures, with a homogeneous appearance and variable possible location (common in the right cardiophrenic angle).

Late gadolinium enhancement CMR imaging is the most sensitive technique in the detection of thrombi in dysfunctional LV and should be favored over echocardiography for this application.<sup>115</sup> Thrombi area avascular structures typically show a complete absence of gadolinium accumulation. This behavior in postcontrast images may be useful when an atrial tumor (generally a myxoma in the left atrium) needs to be differentiated from a possible thrombus.<sup>116</sup> The so-called pseudo-masses, which are normal anatomical variants mimicking a mass, such as false tendons, persistent venous valves and the

Fig. 4



A case of left atrial myxoma in steady-state free precession, T2 STIR and LGE images. Myxoma is globally hyperintense in both steady-state free precession and T2 STIR with peripheral areas of hypointensity due to calcification or hemorrhage and with signal enhancement at LGE.

crista terminalis, can be easily differentiated from pathological cardiac masses using CMR techniques.

#### Differential diagnosis between benign versus malignant masses

Malignant tumors often have typical features on CMR images: common appearance as a broad-based bulky mass with indistinct margins (usually >5 cm in size); signal heterogeneity on different scan sequences, generated by the possible presence of areas of necrosis and hemorrhage; infiltrative signs (i.e. annular or tissue plane crossing within the heart, coexistent involvement of cardiac and extracardiac structures and vascular invasion); signal enhancement during first-pass perfusion and at LGE, with areas of necrosis and hemorrhage; and metastatic lesions observed in other organs. However, the absence of these morphologic elements does not necessarily exclude the detection of malignant tissue by histology, and therefore the ability to distinguish benign from malignant cardiac tumors with CMR is only moderate.<sup>116,117</sup> Associated findings may include pleural or pericardial effusion, that is common with malignant masses and infrequent with benign neoplasms and nonneoplastic conditions.

#### Advantages of cardiac magnetic resonance versus other imaging modalities

CMR provides images at good spatial and temporal resolution that allow definition of the anatomical extent of a mass involving cardiac and/or extracardiac structures, with the possibility to assess any associated functional consequence. Unlike echocardiography, there are no limitations with regard to imaging windows, field of view or assessment of the right heart involvement. CT has some major disadvantages represented by the use of ionizing radiation and the need for iodinated contrast media, with associated risk of nephrotoxicity and potential higher risk for allergic reactions. A major advantage of CMR is a better capacity to perform tissue characterization over both echocardiography and cardiac CT. However, when compared with CMR, echocardiography is less expensive and more available, whereas cardiac CT

allows faster acquisition sessions (few seconds versus 30–45 min) and is able to demonstrate calcification.

#### Congenital heart disease

Congenital heart diseases (CHD) are the main congenital diseases present at birth. Echocardiography remains the first diagnostic tool for CHD evaluation; however, over the past decades, clinical indications for CMR are rapidly evolving due to its capability to provide invaluable cardiac anatomical and functional information.<sup>118–120</sup> CMR approach in pediatric CHD is particularly challenging and needs to be adapted to patient size and heart<sup>121</sup>; moreover, in children less than 8 years old, deep sedation or anesthesia is necessary. Strategy of sedation/anesthesia depends on center availability and expertise.<sup>122–124</sup> Breath hold sequences are generally preferred but, in small children or in deep sedation, free-breathing scan may be the only option. In this case, artifacts from respiratory motion are usually minimized using multiple averages (or number of excitations) or by a diaphragm tracking using navigator algorithm.

Detailed CMR protocols for each CHD is beyond the scope of this article and have been published elsewhere.<sup>120,125,126</sup> In this paragraph, we would like to highlight the asset of CMR for preprocedural and post-procedural evaluation of CHD and appropriate indications criteria.

#### How to scan a patient with a congenital heart disease

Anatomical details are best seen using FSE pulse sequence because of higher resolution than cine imaging and less susceptibility to the artifacts caused by metallic implants. However, SSFP sequence is most frequently used in CHD due to faster acquisition and the possibility to assess regional wall motion, flow turbulences and for functional assessment. The thickness, field of view and voxel size have to be adjusted to patients size and heart rate, an in-plane resolution of 1.2–2 mm and slice thickness of 4–6 mm are recommended in infant and small children.<sup>121</sup> Free-breathing three-dimensional whole-

heart SSFP sequence may be used to obtain a first assessment of cardiac without the need of contrast agents and to plan the rest of the examination in patients with complex anatomy. Three-dimensional whole-heart 'time-of-flight' (TOF) images covering the thorax from the aortic arch to the diaphragm may be a valid alternative of three-dimensional SSFP in presence of flow and motion artifact. However, TOF images are very time expensive, requiring several minutes of acquisition time. Contrast-enhanced magnetic resonance (MR) angiography is routinely used in CHD for the evaluation of vessels anatomy.<sup>127</sup> The timing of image acquisition is tailored to the vessels that need to be assessed, and an appropriate spatial resolution has to be adjusted according to patient size.

Flow assessments in CHD are one of the most important assets of CMR and are performed by means of an acquisition of so-called velocity encoded phase contrast (VEPC) pulse sequences. Clinical applications include measurement of shunt ( $Q_p/Q_s$ ), lung perfusion, cardiac output, valvular regurgitation (mainly semilunar valves), intracardiac baffles and aortopulmonary collateral flow.<sup>128–130</sup> Free-breathing acquisition with multiple average signals are advised to reduce respiratory motion. Common pitfalls of VEPC are misalignment with flow, turbulent flow, malpositioning with regard to valve plane, through plane motion, effects of breathing, effects of eddy currents and other artifacts, and incorrect setting of velocity encoding.<sup>121</sup> Technical details of VEPC were reported in a recent review of the working group on the 'application of CMR' of the Italian Society of Cardiology.<sup>131</sup> Four-dimensional MR flow is a promising

technique that allows acquisition of blood flow information for all vessels included in the three-dimensional imaging volume at the same time under the same physiological status.<sup>132</sup>

LGE is usually performed in adult CHD because the presence of myocardial fibrosis has been demonstrated to be associated with adverse cardiac event,<sup>133,134</sup> although the complete physiopathology is not yet elucidated.

*Potential advantages of CMR versus other imaging modality:*

Transthoracic echocardiography is the first-line tool for the diagnosis and follow-up of patients with CHD due to its low cost, widespread diffusion, portability, ease of use and excellent temporal–spatial resolution. However, its diagnostic utility diminishes with the growth and after surgical procedures. Moreover, echocardiography has limited value for the evaluation of extracardiac structures. Diagnostic cardiac catheterization carries risk of complications and is associated with radiation exposure; furthermore, as a projection technique, it is limited in providing accurate anatomical information. The accuracy of CT in the evaluation of thoracic vessels and the tracheobronchial tree is now well established. CT scanners are also readily available and easy to use compared with CMR and could be preferred in the anatomical evaluation of sick or instable infant. A major disadvantage of CT, especially in children, is the exposure to ionizing radiation with a potential risk of development of radiation-induced malignancies particularly in children.

Although long-time scan, technically complex and expensive, CMR is an invaluable tool in the prerepair and postrepair CHD thanks to its accuracy in the

**Table 5 Congenital heart disease**

	Appropriateness score	ESC guidelines class of indication	Pulse sequences
Evaluation of cardiac and vascular anatomy	8	–	Cine-bSSFP in short-axis views, axial, coronal and sagittal views FSE in short-axis, axial, coronal and sagittal views
Evaluation of LV volumes, mass and EF in unloaded RV heart	6	–	Cine-bSSFP in short-axis views
LV volumes, mass and EF in loaded RV heart	8	–	Cine-bSSFP in short-axis views
RV volumes, mass and EF	9	–	Cine-bSSFP in short-axis views
'Single ventricle' volumes, mass and EF	9	–	Cine-bSSFP in short-axis views
Myocardium viability and fibrosis	9	–	LGE in short-axis and long-axis views
Flow quantifications of valve regurgitation	7	–	VEPC images acquired at the aortic sinotubular junction or at the mid-pulmonary artery Cine-bSSFP in short-axis views
Shunt quantification	9	–	VEPC images acquired at the aortic sinotubular junction and at the mid-pulmonary artery Cine-bSSFP in short-axis views
Atrioventricular morphology	4	–	Cine-bSSFP in short-axis views
Atrioventricular regurgitation	6	–	Cine-bSSFP in short-axis views
Atrioventricular valve stenosis	3	–	Cine-bSSFP in short-axis views
Semilunar valve morphology	6	–	Cine-bSSFP covering aortic or pulmonary root

EF, ejection fraction; bSSFP, balanced Steady State Free Precession; FSE, fast spin echo; LV, left ventricle; RV, right ventricle; VEPC, velocity encoded phase contrast. Appropriateness criteria: 1-3 inappropriate; 4-6 uncertain; 7-9 appropriate.

assessment of biventricular volumes, function, myocardial viability and fibrosis; ability to assess intracardiac and extracardiac anatomy with multiplanar and three-dimensional reconstruction; and accurate quantification of blood flow volume without any spatial limitation. Moreover, CMR is noninvasive nonionizing tool and therefore is suitable for follow-up evaluation of CHD.

*Appropriate use criteria in preoperative and postoperative CHD:* Because of the wide range of clinical and hemodynamical findings in prerepair and in postrepair CHD, we chose to propose appropriate use criteria for specific information commonly addressed to CMR or other imaging tool rather than in each single CHD (Table 5).

## Acknowledgements

*There are no conflicts of interest.*

## References

- 1 Caforio AL, Pankuweit S, Arbustini E, *et al.*, European Society of Cardiology Working Group on Myocardial, Pericardial Diseases. Current state of knowledge on aetiology, diagnosis, management, and therapy of myocarditis: a position statement of the European Society of Cardiology Working Group on Myocardial and Pericardial Diseases. *Eur Heart J* 2013; **34**:2636–2648.
- 2 Di Bella G, Florian A, Oreto L, *et al.* Electrocardiographic findings and myocardial damage in acute myocarditis detected by cardiac magnetic resonance. *Clin Res Cardiol* 2012; **101**:617–624.
- 3 Di Bella G, de Gregorio C, Minutoli F, *et al.* Early diagnosis of focal myocarditis by cardiac magnetic resonance. *Int J Cardiol* 2007; **117**:280–281.
- 4 Friedrich MG, Sechtem U, Schulz-Menger J, *et al.*, International Consensus Group on Cardiovascular Magnetic Resonance in Myocarditis. Cardiovascular magnetic resonance in myocarditis: a JACC White Paper. *J Am Coll Cardiol* 2009; **53**:1475–1487.
- 5 Zagrosek A, Abdel-Aty H, Boyé P, *et al.* Cardiac magnetic resonance monitors reversible and irreversible myocardial injury in myocarditis. *JACC Cardiovasc Imaging* 2009; **2**:131–138.
- 6 Laissy JP, Messin B, Varenne O, *et al.* MRI of acute myocarditis: a comprehensive approach based on various imaging sequences. *Chest* 2002; **122**:1638–1648.
- 7 Kellman P, Aletras AH, Mancini C, *et al.* T2-prepared SSFP improves diagnostic confidence in edema imaging in acute myocardial infarction compared to turbo spin echo. *Magn Reson Med* 2007; **57**:891–897.
- 8 Perfetti M, Malatesta G, Alvarez I, *et al.* A fast and effective method to assess myocardial hyperemia in acute myocarditis by magnetic resonance. *Int J Cardiovasc Imaging* 2014; **30**:629–637.
- 9 Francone M, Chimenti C, Galea N, *et al.* CMR sensitivity varies with clinical presentation and extent of cell necrosis in biopsy-proven acute myocarditis. *JACC Cardiovasc Imaging* 2014; **7**:254–263.
- 10 Gutberlet M, Spors B, Thoma T, *et al.* Suspected chronic myocarditis at cardiac MR: diagnostic accuracy and association with immunohistologically detected inflammation and viral persistence. *Radiology* 2008; **246**:401–409.
- 11 Voigt A, Elgeti T, Durmus T, *et al.* Cardiac magnetic resonance imaging in dilated cardiomyopathy in adults – towards identification of myocardial inflammation. *Eur Radiol* 2011; **21**:925–935.
- 12 De Cobelli F, Pieroni M, Esposito A. Delayed gadolinium-enhanced cardiac magnetic resonance in patients with chronic myocarditis presenting with heart failure or recurrent arrhythmias. *J Am Coll Cardiol* 2006; **47**:1649–1654.
- 13 Mavrogeni S, Spargias C, Bratis C, *et al.* Myocarditis as a precipitating factor for heart failure: evaluation and 1-year follow-up using cardiovascular magnetic resonance and endomyocardial biopsy. *Eur J Heart Fail* 2011; **13**:830–837.
- 14 Mahrholdt H, Wagner A, Deluigi CC, *et al.* Presentation, patterns of myocardial damage, and clinical course of viral myocarditis. *Circulation* 2006; **114**:1581–1615.
- 15 Jeserich M, Konstantinides S, Pavlik G, *et al.* Noninvasive imaging in the diagnosis of acute viral myocarditis. *Clin Res Cardiol* 2009; **98**:753–763.
- 16 Kindermann I, Barth C, Mahfoud F, *et al.* Update on myocarditis. *J Am Coll Cardiol* 2012; **59**:779–792.
- 17 Di Bella G, Gaeta M, Todaro MC, *et al.* Early use of cardiac magnetic resonance reduces hospitalization time and costs in patients with acute myocarditis and preserved left ventricular function: a single center experience. *J Cardiovasc Med (Hagerstown)* 2011; **12**:493–497.
- 18 Bogaert J, Francone M. Cardiovascular magnetic resonance in pericardial diseases. *J Cardiovasc Magn Reson* 2009; **11**:14.
- 19 Zurick AO, Bolen MA, Kwon DH, *et al.* Pericardial delayed hyperenhancement with CMR imaging in patients with constrictive pericarditis undergoing surgical pericardiectomy: a case series with histopathological correlation. *JACC Cardiovasc Imaging* 2011; **4**:1180–1191.
- 20 Alraies MC, AlJaroudi W, Yarmohammadi H, *et al.* Usefulness of cardiac magnetic resonance-guided management in patients with recurrent pericarditis. *Am J Cardiol* 2015; **115**:542–547.
- 21 Oh KY, Shimizu M, Edwards WD, *et al.* Surgical pathology of the parietal pericardium: a study of 344 cases (1993–1999). *Cardiovascul Pathol* 2001; **10**:157–168.
- 22 Adler Y, Charron P, Imazio M, *et al.*, Authors/Task Force Members. 2015 ESC guidelines for the diagnosis and management of pericardial diseases: The Task Force for the Diagnosis and Management of Pericardial Diseases of the European Society of Cardiology (ESC) Endorsed by: The European Association for Cardio-Thoracic Surgery (EACTS). *Eur Heart J* 2015; **36**:2921–2964.
- 23 Aquaro GD, Barison A, Cagnolo A, *et al.* Role of tissue characterization by cardiac magnetic resonance in the diagnosis of constrictive pericarditis. *Int J Cardiovasc Imaging* 2015; **31**:1021–1031.
- 24 Assomull RG, Shakespeare C, Kalra PR, *et al.* Role of cardiovascular magnetic resonance as a gatekeeper to invasive coronary angiography in patients presenting with heart failure of unknown etiology. *Circulation* 2011; **124**:1351–1360.
- 25 Calore C, Cacciavillani L, Boffa GM, *et al.* Contrast-enhanced cardiovascular magnetic resonance in primary and ischemic dilated cardiomyopathy. *J Cardiovasc Med* 2007; **8**:821–829.
- 26 Won E, Donnino R, Srichai MB, *et al.* Diagnostic accuracy of cardiac magnetic resonance imaging in the evaluation of newly diagnosed heart failure with reduced left ventricular ejection fraction. *Am J Cardiol* 2015; **116**:1082–1087.
- 27 Assomull RG, Prasad SK, Lyne J, *et al.* Cardiovascular magnetic resonance, fibrosis, and prognosis in dilated cardiomyopathy. *J Am Coll Cardiol* 2006; **48**:1977–1985.
- 28 Masci PG, Doulatpis C, Bertella E, *et al.* Incremental prognostic value of myocardial fibrosis in patients with nonischemic cardiomyopathy without congestive heart failure. *Circ Heart Fail* 2014; **7**:448–456.
- 29 Perazzolo Marra M, De Lazzari M, Zorzi A, *et al.* Impact of the presence and amount of myocardial fibrosis by cardiac magnetic resonance on arrhythmic outcome and sudden cardiac death in nonischemic dilated cardiomyopathy. *Heart Rhythm* 2014; **11**:856–863.
- 30 Kuruvilla S, Adenaw N, Katwal AB, *et al.* Late gadolinium enhancement on cardiac magnetic resonance predicts adverse cardiovascular outcomes in nonischemic cardiomyopathy: a systematic review and meta-analysis. *Circ Cardiovasc Imaging* 2014; **7**:250–258.
- 31 Marcus FI, McKenna WJ, Sherrill D, *et al.* Diagnosis of arrhythmogenic right ventricular cardiomyopathy/dysplasia: proposed modification of the Task Force Criteria. *Circulation* 2010; **121**:1533–1541.
- 32 Tandri H, Castillo E, Ferrari VA, *et al.* Magnetic resonance imaging of arrhythmogenic right ventricular dysplasia: sensitivity, specificity, and observer variability of fat detection versus functional analysis of the right ventricle. *J Am Coll Cardiol* 2006; **48**:2277–2284; 23.
- 33 Marcus F, Basso C, Gear K, Sorrell VL. Pitfalls in the diagnosis of arrhythmogenic right ventricular cardiomyopathy/dysplasia. *Am J Cardiol* 2010; **105**:1036–1039; 44.
- 34 Tandri H, Calkins H, Nasir K, *et al.* Magnetic resonance imaging findings in patients meeting task force criteria for arrhythmogenic right ventricular dysplasia. *J Cardiovasc Electrophysiol* 2003; **14**:476–482.
- 35 Perazzolo Marra M, Rizzo S, Bauce B, *et al.* Arrhythmogenic right ventricular cardiomyopathy. Contribution of cardiac magnetic resonance imaging to the diagnosis. *Herz* 2015; **40**:600–606.
- 36 Zimmerman S. Arrhythmogenic right ventricular right cardiomyopathy / dysplasia. An updated imaging approach. *Magn Reson Imaging Clin N Am* 2015; **23**:69–79.
- 37 te Riele AS, Tandri H, Bluemke DA. Arrhythmogenic right ventricular cardiomyopathy (ARVC): cardiovascular magnetic resonance update. *J Cardiovasc Magn Reson* 2014; **16**:50.
- 38 Chahal H, Johnson C, Tandri H, *et al.* Relation of cardiovascular risk factors to right ventricular structure and function as determined by magnetic resonance imaging (results from the multiethnic study of atherosclerosis). *Am J Cardiol* 2010; **106**:110–116.

- 39 Malayeri AA, Johnson WC, Macedo R, *et al.* Cardiac cine MRI: quantification of the relationship between fast gradient echo and steady-state free precession for determination of myocardial mass and volumes. *J Magn Reson Imaging* 2008; **28**:60–66.
- 40 Moon JC, Lorenz CH, Francis JM, *et al.* Breath-hold FLASH and FISP cardiovascular MR imaging: left ventricular volume differences and reproducibility. *Radiology* 2002; **223**:789–797.
- 41 Aquaro GD, Pingitore A, Strata E, *et al.* Cardiac magnetic resonance predicts outcome in patients with premature ventricular complexes of left bundle branch block morphology. *J Am Coll Cardiol* 2010; **56**:1235–1243.
- 42 Deac M, Alpendurada F, Fanaie F, *et al.* Prognostic value of cardiovascular magnetic resonance in patients with suspected arrhythmogenic right ventricular cardiomyopathy. *Int J Cardiol* 2013; **168**:3514–3521.
- 43 Falk RH, Comenzo RL, Skinner M. The systemic amyloidoses. *N Engl J Med* 1997; **337**:898–909.
- 44 Rapezzi C, Merlini G, Quarta CC, *et al.* Systemic cardiac amyloidoses: disease profiles and clinical courses of the 3 main types. *Circulation* 2009; **120**:1203–1212.
- 45 Dubrey SW, Cha K, Skinner M, *et al.* Familial and primary (AL) cardiac amyloidosis: echocardiographically similar diseases with distinctly different clinical outcomes. *Heart* 1997; **78**:74–82.
- 46 Quarta CC, Solomon SD, Uraizee I, *et al.* Left ventricular structure and function in transthyretin-related versus light-chain cardiac amyloidosis. *Circulation* 2014; **129**:1840–1849.
- 47 Fontana M, Banyersad SM, Treibel TA, *et al.* Differential myocyte responses in patients with cardiac transthyretin amyloidosis and light-chain amyloidosis: a cardiac MR imaging study. *Radiology* 2015; **277**:388–397.
- 48 Pozo E, Kanwar A, Deochand R, *et al.* Cardiac magnetic resonance evaluation of left ventricular remodelling distribution in cardiac amyloidosis. *Heart* 2014; **100**:1688–1695.
- 49 Maceira AM, Joshi J, Prasad SK, *et al.* Cardiovascular magnetic resonance in cardiac amyloidosis. *Circulation* 2005; **111**:186–193.
- 50 Vogelsberg H, Mahrholdt H, Deluigi CC, *et al.* Cardiovascular magnetic resonance in clinically suspected cardiac amyloidosis: noninvasive imaging compared to endomyocardial biopsy. *J Am Coll Cardiol* 2008; **51**:1022–1030.
- 51 Aquaro GD, Pugliese NR, Perfetto F, *et al.* Myocardial signal intensity decay after gadolinium injection: a fast and effective method for the diagnosis of cardiac amyloidosis. *Int J Cardiovasc Imaging* 2014; **30**:1105–1115.
- 52 Syed IS, Glockner JF, Feng D, *et al.* Role of cardiac magnetic resonance imaging in the detection of cardiac amyloidosis. *JACC Cardiovasc Imaging* 2010; **3**:155–164.
- 53 Austin BA, Tang WH, Rodriguez ER, *et al.* Delayed hyper-enhancement magnetic resonance imaging provides incremental diagnostic and prognostic utility in suspected cardiac amyloidosis. *JACC Cardiovasc Imaging* 2009; **2**:1369–1377.
- 54 Dungu JN, Valencia O, Pinney JH, *et al.* CMR-based differentiation of AL and ATTR cardiac amyloidosis. *JACC Cardiovasc Imaging* 2014; **7**:133–142.
- 55 Fontana M, Chung R, Hawkins PN, Moon JC. Cardiovascular magnetic resonance for amyloidosis. *Heart Fail Rev* 2015; **20**:133–144.
- 56 Fontana M, Pica S, Reant P, *et al.* Prognostic value of late gadolinium enhancement cardiovascular magnetic resonance in cardiac amyloidosis. *Circulation* 2015; **132**:1570–1579.
- 57 Karamitsos TD, Piechnik SK, Banyersad SM, *et al.* Noncontrast T1 mapping for the diagnosis of cardiac amyloidosis. *JACC Cardiovasc Imaging* 2013; **6**:488–497.
- 58 Banyersad SM, Sado DM, Flett AS, *et al.* Quantification of myocardial extracellular volume fraction in systemic AL amyloidosis: an equilibrium contrast cardiovascular magnetic resonance study. *Circ Cardiovasc Imaging* 2013; **6**:34–39.
- 59 Banyersad SM, Fontana M, Maestrini V, *et al.* T1 mapping and survival in systemic light-chain amyloidosis. *Eur Heart J* 2015; **36**:244–251.
- 60 Fontana M, Banyersad SM, Treibel TA, *et al.* Native T1 mapping in transthyretin amyloidosis. *JACC Cardiovasc Imaging* 2014; **7**:157–165.
- 61 Barison A, Aquaro GD, Pugliese NR, *et al.* Measurement of myocardial amyloid deposition in systemic amyloidosis: insights from cardiovascular magnetic resonance imaging. *J Intern Med* 2015; **277**:605–614.
- 62 Gersh BJ, Maron BJ, Bonow RO, *et al.* 2011 ACCF/AHA guideline for the diagnosis and treatment of hypertrophic cardiomyopathy: a report of the American College of Cardiology Foundation/American Heart Association Task Force on Practice Guidelines. *Circulation* 2011; **124**:e783–e831.
- 63 Elliott PM, Anastakis A, Borger MA, *et al.*, Authors/Task Force members. 2014 ESC guidelines on diagnosis and management of hypertrophic cardiomyopathy: the Task Force for the Diagnosis and Management of Hypertrophic Cardiomyopathy of the European Society of Cardiology (ESC). *Eur Heart J* 2014; **35**:2733–2779.
- 64 Maron MS, Hauser TH, Dubrow E, *et al.* Right ventricular involvement in hypertrophic cardiomyopathy. *Am J Cardiol* 2007; **100**:1293–1298.
- 65 Rickers C, Wilke NM, Jerosch-Herold M, *et al.* Utility of cardiac magnetic resonance imaging in the diagnosis of hypertrophic cardiomyopathy. *Circulation* 2005; **112**:855–861.
- 66 Maron MS, Maron BJ, Harrigan C, *et al.* Hypertrophic cardiomyopathy phenotype revisited after 50 years with cardiovascular magnetic resonance. *J Am Coll Cardiol* 2009; **54**:220–228.
- 67 Moon JC, Fisher NG, McKenna WJ, Pennell DJ. Detection of apical hypertrophic cardiomyopathy by cardiovascular magnetic resonance in patients with nondiagnostic echocardiography. *Heart* 2004; **90**:645–649.
- 68 Fattori R, Biagini E, Lorenzini M, *et al.* Significance of magnetic resonance imaging in apical hypertrophic cardiomyopathy. *Am J Cardiol* 2010; **105**:1592–1596.
- 69 Maron MS, Finley JJ, Bos JM, *et al.* Prevalence, clinical significance, and natural history of left ventricular apical aneurysms in hypertrophic cardiomyopathy. *Circulation* 2008; **118**:1541–1549.
- 70 Harrigan CJ, Appelbaum E, Maron BJ, *et al.* Significance of papillary muscle abnormalities identified by cardiovascular magnetic resonance in hypertrophic cardiomyopathy. *Am J Cardiol* 2008; **101**:668–673.
- 71 Kwon DH, Setser RM, Thamilarasan M, *et al.* Abnormal papillary muscle morphology is independently associated with increased left ventricular outflow tract obstruction in hypertrophic cardiomyopathy. *Heart* 2008; **94**:1295–1301.
- 72 Germans T, Wilde AA, Dijkmans PA, *et al.* Structural abnormalities of the inferoseptal left ventricular wall detected by cardiac magnetic resonance imaging in carriers of hypertrophic cardiomyopathy mutations. *J Am Coll Cardiol* 2006; **48**:2518–2523.
- 73 Brouwer WP, Germans T, Head MC, *et al.* Multiple myocardial crypts on modified long-axis view are a specific finding in pre-hypertrophic HCM mutation carriers. *Eur Heart J Cardiovasc Imaging* 2012; **13**:292–297.
- 74 Maron MS, Rowin EJ, Lin D, *et al.* Prevalence and clinical profile of myocardial crypts in hypertrophic cardiomyopathy. *Circ Cardiovasc Imaging* 2012; **5**:441–447.
- 75 Deva DP, Williams LK, Care M, *et al.* Deep basal inferoseptal crypts occur more commonly in patients with hypertrophic cardiomyopathy due to disease-causing myofibrillar mutations. *Radiology* 2013; **269**:68–76.
- 76 Maron MS, Olivetto I, Harrigan C, *et al.* Mitral valve abnormalities identified by cardiovascular magnetic resonance represent a primary phenotypic expression of hypertrophic cardiomyopathy. *Circulation* 2011; **124**:40–47.
- 77 Captur G, Lopes LR, Mohun TJ, *et al.* Prediction of sarcomere mutations in subclinical hypertrophic cardiomyopathy. *Circ Cardiovasc Imaging* 2014; **7**:863–871.
- 78 Captur G, Lopes LR, Patel V, *et al.* Abnormal cardiac formation in hypertrophic cardiomyopathy: fractal analysis of trabeculae and preclinical gene expression. *Circ Cardiovasc Genet* 2014; **7**:241–248.
- 79 Yuan J, Qiao S, Zhang Y, *et al.* Follow-up by cardiac magnetic resonance imaging in patients with hypertrophic cardiomyopathy who underwent percutaneous ventricular septal ablation. *Am J Cardiol* 2010; **106**:1487–1491.
- 80 van Dockum WG, ten Cate FJ, ten Berg JM, *et al.* Myocardial infarction after percutaneous transluminal septal myocardial ablation in hypertrophic obstructive cardiomyopathy: evaluation by contrast-enhanced magnetic resonance imaging. *J Am Coll Cardiol* 2004; **43**:27–34.
- 81 Valeti US, Nishimura RA, Holmes DR, *et al.* Comparison of surgical septal myectomy and alcohol septal ablation with cardiac magnetic resonance imaging in patients with hypertrophic obstructive cardiomyopathy. *J Am Coll Cardiol* 2007; **49**:350–357.
- 82 Moon JC, Reed E, Sheppard MN, *et al.* The histologic basis of late gadolinium enhancement cardiovascular magnetic resonance in hypertrophic cardiomyopathy. *J Am Coll Cardiol* 2004; **43**:2260–2264.
- 83 Rudolph A, Abdel-Aty H, Bohl S, *et al.* Noninvasive detection of fibrosis applying contrast-enhanced cardiac magnetic resonance in different forms of left ventricular hypertrophy relation to remodeling. *J Am Coll Cardiol* 2009; **53**:284–291.
- 84 Choudhury L, Mahrholdt H, Wagner A, *et al.* Myocardial scarring in asymptomatic or mildly symptomatic patients with hypertrophic cardiomyopathy. *J Am Coll Cardiol* 2002; **40**:2156–2164.
- 85 Maron MS, Appelbaum E, Harrigan CJ, *et al.* Clinical profile and significance of delayed enhancement in hypertrophic cardiomyopathy. *Circ Heart Fail* 2008; **1**:184–191.
- 86 Rubinshtein R, Glockner JF, Ommen SR, *et al.* Characteristics and clinical significance of late gadolinium enhancement by contrast-enhanced magnetic resonance imaging in patients with hypertrophic cardiomyopathy. *Circ Heart Fail* 2010; **3**:51–58.

- 87 Bruder O, Wagner A, Jensen CJ, *et al.* Myocardial scar visualized by cardiovascular magnetic resonance imaging predicts major adverse events in patients with hypertrophic cardiomyopathy. *J Am Coll Cardiol* 2010; **56**:875–887.
- 88 O'Hanlon R, Grasso A, Roughton M, *et al.* Prognostic significance of myocardial fibrosis in hypertrophic cardiomyopathy. *J Am Coll Cardiol* 2010; **56**:867–874.
- 89 Chan RH, Maron BJ, Olivetto I, *et al.* Prognostic value of quantitative contrast-enhanced cardiovascular magnetic resonance for the evaluation of sudden death risk in patients with hypertrophic cardiomyopathy. *Circulation* 2014; **130**:484–495.
- 90 Moon JC, Sheppard M, Reed E, *et al.* The histological basis of late gadolinium enhancement cardiovascular magnetic resonance in a patient with Anderson–Fabry disease. *J Cardiovasc Magn Reson* 2006; **8**:479–482.
- 91 Moon JC, Sachdev B, Elkington AG, *et al.* Gadolinium enhanced cardiovascular magnetic resonance in Anderson–Fabry disease: evidence for a disease specific abnormality of the myocardial interstitium. *Eur Heart J* 2003; **24**:2151–2155.
- 92 De Cobelli F, Esposito A, Belloni E, *et al.* Delayed-enhanced cardiac MRI for differentiation of Fabry's disease from symmetric hypertrophic cardiomyopathy. *AJR Am J Roentgenol* 2009; **192**:W97–W102.
- 93 Sado DM, White SK, Piechnik SK, *et al.* Identification and assessment of Anderson–Fabry disease by cardiovascular magnetic resonance noncontrast myocardial T1 mapping. *Circ Cardiovasc Imaging* 2013; **6**:392–398.
- 94 Pica S, Sado DM, Maestrini V, *et al.* Reproducibility of native myocardial T1 mapping in the assessment of Fabry disease and its role in early detection of cardiac involvement by cardiovascular magnetic resonance. *J Cardiovasc Magn Reson* 2014; **16**:99.
- 95 Thompson RB, Chow K, Khan A, *et al.* T1 mapping with cardiovascular MRI is highly sensitive for Fabry disease independent of hypertrophy and sex. *Circ Cardiovasc Imaging* 2013; **6**:637–645.
- 96 Meloni A, Positano V, Ruffo GB, *et al.* Improvement of heart iron with preserved patterns of iron store by CMR-guided chelation therapy. *Eur Heart J Cardiovasc Imaging* 2015; **16**:325–334.
- 97 Carpenter JP, He T, Kirk P, *et al.* On T2\* magnetic resonance and cardiac iron. *Circulation* 2011; **123**:1519–1528.
- 98 Pepe A, Meloni A, Capra M, *et al.* Deferasirox, deferiprone and desferrioxamine treatment in thalassemia major patients: cardiac iron and function comparison determined by quantitative magnetic resonance imaging. *Haematologica* 2011; **96**:41–47.
- 99 Pepe A, Positano V, Santarelli MF, *et al.* Multislice multiecho T2\* cardiovascular magnetic resonance for detection of the heterogeneous distribution of myocardial iron overload. *J Magn Reson Imaging* 2006; **23**:662–668.
- 100 Casale M, Meloni A, Filosa A, *et al.* Multiparametric cardiac magnetic resonance survey in children with thalassemia major: a multicenter study. *Circ Cardiovasc Imaging* 2015; **8**:e003230; doi: 10.1161/CIRCIMAGING.115003230.
- 101 Borgna-Pignatti C, Meloni A, Guerrini G, *et al.* Myocardial iron overload in thalassaemia major. How early to check? *Br J Haematol* 2014; **164**:579–585.
- 102 Pepe A, Positano V, Capra M, *et al.* Myocardial scarring by delayed enhancement cardiovascular magnetic resonance in thalassaemia major. *Heart* 2009; **95**:1688–1693.
- 103 Oechslin EN, Jost CHA, Rojas JR, *et al.* Long-term follow-up of 34 adults with isolated left ventricular noncompaction: a distinct cardiomyopathy with poor prognosis. *J Am Coll Cardiol* 2000; **36**:493–500.
- 104 Petersen SE, Selvanayagam JB, Wiesmann F, *et al.* Left ventricular noncompaction. Insight from cardiovascular magnetic resonance imaging. *J Am Coll Cardiol* 2005; **46**:101–105.
- 105 Jacquier A, Thuny F, Jop B, *et al.* Measurement of trabeculated left ventricular mass using cardiac magnetic resonance imaging in the diagnosis of left ventricular noncompaction. *Eur Heart J* 2010; **31**:1098–1104.
- 106 Grothoff M, Pachowsky M, Hoffmann J, *et al.* Value of cardiovascular MR in diagnosing left ventricular noncompaction cardiomyopathy and in discriminating between other cardiomyopathies. *Eur Radiol* 2012; **22**:2699–2709.
- 107 Nucifora G, Aquaro GD, Pingitore A, *et al.* Myocardial fibrosis in isolated left ventricular noncompaction and its relation to disease severity. *Eur J Heart Fail* 2011; **13**:170–176.
- 108 Silverman KJ, Hutchins GM, Bulkley BH. Cardiac sarcoid: a clinicopathologic study of 84 unselected patients with systemic sarcoidosis. *Circulation* 1978; **58**:1204–1211.
- 109 Smedema JP, Snoep G, van Kroonenburgh MPG, *et al.* Evaluation of the accuracy of gadolinium enhanced cardiovascular magnetic resonance in the diagnosis of cardiac sarcoidosis. *J Am Coll Cardiol* 2005; **45**:1683–1690.
- 110 Vignaux O. Cardiac sarcoidosis: spectrum of MRI features. *Am J Roentgenol* 2005; **184**:249–254.
- 111 Plana JC, Galderisi M, Barac A, *et al.* Expert consensus for multimodality imaging evaluation of adult patients during and after cancer therapy: a report from the American Society of Echocardiography and the European Association of Cardiovascular Imaging. *Eur Heart J Cardiovasc Imaging* 2015; **15**:1063–1093.
- 112 Naruse Y, Sato A, Kasahara K, *et al.* The clinical impact of late gadolinium enhancement in Takotsubo cardiomyopathy; serial analysis of cardiovascular magnetic resonance images. *J Cardiovasc Magn Reson* 2011; **13**:67.
- 113 Motwani M, Kidambi A, Herzog BA, *et al.* MR imaging of cardiac tumors and masses: a review of methods and clinical applications. *Radiology* 2013; **268**:26–43.
- 114 Butany J, Leong SW, Carmichael K, Komeda M. A 30-year analysis of cardiac neoplasms at autopsy. *Can J Cardiol* 2005; **21**:675–680.
- 115 Fussen S, De Boeck BW, Zellweger MJ, *et al.* Cardiovascular magnetic resonance imaging for diagnosis and clinical management of suspected cardiac masses and tumours. *Eur Heart J* 2011; **32**:1551–1560.
- 116 Roifman I, Connelly KA, Wright GA, Wijeyesundera HC. Echocardiography vs. cardiac magnetic resonance imaging for the diagnosis of left ventricular thrombus: a systematic review. *Can J Cardiol* 2015; **31**:785–791.
- 117 Pazos-López P, Pozo E, Siqueira ME, *et al.* Value of CMR for the differential diagnosis of cardiac masses. *JACC Cardiovasc Imaging* 2014; **7**:896–905.
- 118 Beroukhim RS, Prakash A, Buechel ER, *et al.* Characterization of cardiac tumors in children by cardiovascular magnetic resonance imaging: a multicenter experience. *J Am Coll Cardiol* 2011; **58**:1044–1054.
- 119 Weber OM, Higgins CB. MR evaluation of cardiovascular physiology in congenital heart disease: flow and function. *J Cardiovasc Magn Reson* 2006; **8**:607–617.
- 120 Fratz S, Hess J, Schuhbaeck A, *et al.* Routine clinical cardiovascular magnetic resonance in paediatric and adult congenital heart disease: patients, protocols, questions asked and contributions made. *J Cardiovasc Magn Reson* 2008; **10**:46.
- 121 Bailliar F, Hughes ML, Taylor AM. Introduction to cardiac imaging in infants and children: techniques, potential, and role in the imaging work-up of various cardiac malformations and other pediatric heart conditions. *Eur J Radiol* 2008; **68**:191–198.
- 122 Fratz S, Chung T, Greil G, *et al.* Guidelines and protocols for cardiovascular magnetic resonance in children and adults with congenital heart disease: SCMR expert consensus group on congenital heart disease. *J Cardiovasc Magn Reson* 2013; **15**:51.
- 123 Odegard KC, DiNardo JA, Tsai-Goodman B, *et al.* Anaesthesia considerations for cardiac MRI in infants and small children. *Paediatr Anaesth* 2004; **14**:471–476.
- 124 Osborn I. Magnetic resonance imaging anesthesia: new challenges and techniques. *Curr Opin Anaesthesiol* 2002; **15**:443–448.
- 125 Fogel MA, Weinberg PM, Parave E, *et al.* Deep sedation for cardiac magnetic resonance imaging: a comparison with cardiac anesthesia. *J Pediatr* 2008; **152**:534–539; 539.e1.
- 126 Kilner PJ, Geva T, Kaemmerer H, *et al.* Recommendations for cardiovascular magnetic resonance in adults with congenital heart disease from the respective working groups of the European Society of Cardiology. *Eur Heart J* 2010; **31**:794–805.
- 127 Corno AF, Festa GP. Introduction to CT scan and MRI Congenital heart defects: decision making for cardiac surgery, Volume 3 CT-scan and MRI. *Springer* 2009; **3**:1–17.
- 128 Valsangiaco Buchel ER, DiBernardo S, Bauersfeld U, Berger F. Contrast-enhanced magnetic resonance angiography of the great arteries in patients with congenital heart disease: an accurate tool for planning catheter-guided interventions. *Int J Cardiovasc Imaging* 2005; **21**:313–322.
- 129 Beerbaum P, Korperich H, Barth P, *et al.* Noninvasive quantification of left-to-right shunt in pediatric patients: phase-contrast cine magnetic resonance imaging compared with invasive oximetry. *Circulation* 2001; **103**:2476–2482.
- 130 Powell AJ, Tsai-Goodman B, Prakash A, *et al.* Comparison between phase-velocity cine magnetic resonance imaging and invasive oximetry for quantification of atrial shunts. *Am J Cardiol* 2003; **91**:1523–1525.

- 131 Rebergen SA, Chin JG, Ottenkamp J, *et al.* Pulmonary regurgitation in the late postoperative follow-up of tetralogy of Fallot. Volumetric quantitation by nuclear magnetic resonance velocity mapping. *Circulation* 1993; **88**:2257–2266.
- 132 Aquaro GD, Barison A, Todiere G, *et al.*, working group 'Applicazioni della Risonanza Magnetica' of the Italian Society of Cardiology. Cardiac magnetic resonance 'virtual catheterization' for the quantification of valvular regurgitations and cardiac shunt. *J Cardiovasc Med* 2015; **16**:663–670.
- 133 Vasanawala SS, Hanneman K, Alley MT, Hsiao A. Congenital heart disease assessment with 4D flow MRI. *J Magn Reson Imaging* 2015; **42**:870–886.
- 134 Babu-Narayan SV, Kilner PJ, Li W, *et al.* Ventricular fibrosis suggested by cardiovascular magnetic resonance in adults with repaired tetralogy of fallot and its relationship to adverse markers of clinical outcome. *Circulation* 2006; **113**:405–413.